

Published in final edited form as:

Biomaterials. 2015 April ; 0: 26–34. doi:10.1016/j.biomaterials.2014.12.050.

Localized Delivery of Mechano-Growth Factor E-domain Peptide via Polymeric Microstructures Improves Cardiac Function following Myocardial Infarction

James R. Peña¹, James Pinney³, Perla Ayala², Tejal Desai^{2,4}, and Paul H. Goldspink¹

¹Department of Physiology & Cardiovascular Center, Medical College of Wisconsin, Milwaukee WI, 53226 USA

²UC Berkeley-UCSF Graduate Group in Bioengineering

³UCSF Medical Scientist Training Program, University of California, San Francisco, San Francisco, CA 94158. USA

⁴Department of Bioengineering and Therapeutic Sciences, University of California, San Francisco, San Francisco, CA 94158. USA

Abstract

The Insulin like growth factor-I isoform mechano-growth factor (MGF), is expressed in the heart following myocardial infarction and encodes a unique E-domain region. To examine E-domain function, we delivered a synthetic peptide corresponding to the unique E-domain region of the human MGF (IGF-1Ec) via peptide eluting polymeric microstructures to the heart. The microstructures were made of poly (ethylene glycol) dimethacrylate hydrogel and bioengineered to be the same size as an adult cardiac myocyte (100×15×15 μm) and with a stiffness of 20 kPa. Peptide eluting microrods and empty microrods were delivered via intramuscular injection following coronary artery ligation in mice. To examine the physiologic consequences, we assessed the impact of peptide delivery on cardiac function and cardiovascular hemodynamics using pressure-volume loops and gene expression by quantitative RT-PCR. A significant decline in both systolic and diastolic function accompanied by pathologic hypertrophy occurred by 2 weeks which decompensated further by 10 weeks post-infarct in the untreated groups. Delivery of the E-domain peptide eluting microrods decreased mortality, ameliorated the decline in hemodynamics, and delayed decompensation. This was associated with the inhibition of pathologic hypertrophy despite increasing vascular impedance. Delivery of the empty microrods had limited effects on hemodynamics and while pathologic hypertrophy persisted there was a decrease in ventricular stiffness. Our data show that cardiac restricted administration of the MGF E-domain peptide using

© 2014 Elsevier Ltd. All rights reserved.

Address for correspondence: Paul H. Goldspink, Ph.D. Department of Physiology & Cardiovascular Center, Medical College of Wisconsin, 8701 Watertown Plank Road, P.O. Box 26509, Milwaukee, WI 53226, Phone: 414-456-7575, Fax: 414-456-6515, pgoldspink@mcw.edu.

There are no conflicts of interest to report for any of the authors.

Publisher's Disclaimer: This is a PDF file of an unedited manuscript that has been accepted for publication. As a service to our customers we are providing this early version of the manuscript. The manuscript will undergo copyediting, typesetting, and review of the resulting proof before it is published in its final citable form. Please note that during the production process errors may be discovered which could affect the content, and all legal disclaimers that apply to the journal pertain.

polymeric microstructures may be used to prevent adverse remodeling of the heart and improve function following myocardial infarction.

Keywords

Growth Factors; Peptide; Polyethylene glycol dimethacrylate; Hydrogel; Photolithography; Drug delivery; Cardiac tissue repair

Introduction

Ischemia that leads to myocardial infarction (MI) causes both structural and functional changes of the heart that contribute to the progression of heart failure. During these events, local growth factors such as IGF-1 are produced by the myocardium to mitigate damage and may have therapeutic potential in the context of heart failure [1,2].

IGF-1 functions as a paracrine and autocrine growth factor that is expressed in numerous tissues mediating regenerative and repair processes [3-5]. The IGF-I gene yields a mature peptide (70 amino acids), but contains several alternatively spliced exons [6,7]. Splicing of exons 4, 5 and 6 gives rise to different E-domains within the propeptide of the various IGF-1 isoforms. Interest has grown with respect to IGF-1 isoform function and the action of their unique E-domains has become the focus of isoform structure/function analysis. Studies have shown that IGF-1 isoforms display different temporal expression dynamics in tissues following injury [8-10]. We have previously reported that the IGF-1 isoform known as Mechano-Growth Factor (MGF), which is equivalent to the rodent IGF-1Eb and human IGF-1Ec, is preferentially expressed in the heart following MI in mice [8]. To ascertain whether the E-domain region of the MGF isoform has biological function, we delivered a stabilized 24-amino acid peptide analog corresponding to the unique carboxyl-terminal sequence to MI mice. Systemic delivery of the MGF E-domain peptide during MI resulted in the preservation of cardiac function, inhibition of myocyte apoptosis and prevention of pathologic remodeling in mice [8]. Likewise, similar cardioprotective effects were obtained with intracoronary delivery of the MGF E-domain peptide independently and synergistically with IGF-1 in an ovine model of MI [11]. Furthermore, neuroprotective activities of the MGF E-domain peptide have been reported in a model of global transient cerebral ischemia and by preventing apoptosis of dopaminergic neurons in response to oxidative stress [12,13].

These prior studies examined the beneficial effects of the stabilized peptide via systemic delivery within the first 2 week of the ischemic insult. To extend these studies, we examined the long-term benefits of MGF E-domain peptide delivery during the acute phase (12 hours) and chronic phase (after 8 weeks) on the decompensated hypertrophic heart in 10 week post-MI mice [14]. Depending on when the E-domain peptide was delivered, analysis showed that the improvements in cardiovascular hemodynamics were associated with either a prevention or delay in decompensation post-MI. In particular, systemic delivery produced a significant reduction in vascular impedance during the chronic phase which reduced afterload on the failing heart and improved ventricular mechanoenergetics. Collectively, these physiologic studies have shown that systemic delivery of the stabilized MGF E-domain peptide produces beneficial cardiovascular effects in rodent and large animals

models of MI, which develop similar pathophysiologic events to those observed in human patients. However, the integrated physiologic response associated with systemic delivery makes it difficult to assess causality. Consequently, we wished to determine whether direct delivery and action of the MGF E-domain peptide to the heart would elicit similar cardiovascular improvements in the rodent model post-MI as previously reported. Accordingly, we developed a novel technology for intramyocardial delivery using poly(ethylene glycol) dimethacrylate peptide eluting microrod scaffolds (MRS), engineered to a size and shape similar to adult cardiac myocytes. We tested whether delivery of the native 24 amino acid non-stabilized MGF E-domain peptide directly to the heart would be sufficient to produce beneficial effects on cardiovascular function and cardiac remodeling post-MI. We examined the physiological consequences of peptide eluting MRS during the development of compensatory hypertrophy (2 week) and following decompensated hypertrophy (10 week) post-MI. We found significant improvements in numerous cardiac functional parameters and attenuation of pathologic remodeling in mice injected with the peptide eluting MRS. Furthermore, we found limited effects on parameters of vascular function indicating the direct actions of the MGF E-domain peptide on the myocardium are sufficient to mitigate damage following MI and improve function.

Materials and Methods

Ethics Statement

The experiments were approved by the Medical College of Wisconsin Institutional Animal Care and Use Committee (IACUC) in accordance with the National Institutes of Health Guide for the Care and Use of Laboratory Animals. Animals were maintained on a 12 hr light/dark cycle with ad libitum access to standard rodent chow and water.

Myocardial infarction

C57BL/6 male mice (20-25g) were anesthetized with 3% isoflurane in a closed induction chamber and injected with Etomidate (20 mg/kg, i.p.). Mice were intubated and connected to a rodent ventilator with a tidal volume of 140-170 μ l at a rate of 130-170 breaths/min (Harvard Apparatus). Surgical anesthesia was regulated by delivery of 1.5% isoflurane through a vaporizer with 95% oxygen and routinely monitored by the toe pinch reflex response. The left anterior descending coronary artery was ligated with 8-0 silk suture 1-2 mm below the left atrium to induce a 45-50% infarct, as previously published [8,14-16]. Two cohorts of mice were used for analysis of cardiac function at 2 and 10 week post-MI. Sham operated mice underwent thoracotomy, pericardial membrane rupture, simulated LAD ligation and intramuscular injection of saline. Treated mice were injected with E-domain peptide eluting MRS (\sim 0.1ng E-domain peptide/rod) or MRS without peptide (empty MRS). Approximately 10^4 PEGDMA microrods in 10 μ l of sterile saline were injected via a 30G needle attached to a 50 μ l Hamilton Gastight syringe mounted on a constant pressure syringe pump (Harvard Apparatus), into 3 regions of the blanched myocardium 10 minutes following coronary artery ligation. An additional 2 week group received an equivalent dose of the E-domain peptide via intramuscular injection (1 μ g).

PEGDMA microrod fabrication

Microrods were fabricated as previously described [17]. Briefly, poly(ethylene glycol) dimethacrylate (PEGDMA) MW 750, photo-initiator 2,2-dimethoxy-2-phenylacetophenone (Sigma) and the 24 amino acid peptide (YQPPSTNKNTKSQRRKGFEEHK), corresponding to the unique C-terminal E-domain of the human MGF isoform (LifeTein, NJ) were dissolved in 1-vinyl-*n*-pyrrolidone crosslinker (100 mg/mL) and 1 × phosphate-buffered saline (PBS). 20 kPa microrods were created by varying the PEGDMA and the photoinitiator-crosslinker concentrations. Photolithography was used to create microrods designed to have the dimensions 100 × 15 × 15 μm, micro-fabricated in 3-inch silicon wafers. The PEGDMA precursor solution was spun onto each wafer to a thickness of 15 μm. The wafer was exposed using a Karl Suss MJB3 mask aligner to a 405 nm light source through the microrod patterned photomask at 9 mW/cm². Microrods on the wafer were rinsed with isopropanol, dried with N₂ gas and removed by rinsing the wafer with 70% ethanol before gently scraping with a cell scraper. The collected microrods were centrifuged and rinsed in 70% ethanol three times before being resuspended in sterile saline. The elution kinetics of the MGF E-domain peptide from these MRS has been shown to be complete (100% eluted) by 2 week *in vitro* [18].

Pressure-volume loops

Under the same anesthetic regiment, a 1.2 French pressure-volume conductance catheter (Scisense Instruments, London, Ontario) was inserted into the right carotid artery to measure baseline arterial pressure, then advanced retrograde into the LV to record baseline hemodynamics in the closed chest configuration with the ADVantage Pressure Volume Conductance System (Scisense Instruments, London, Ontario). A small incision in the abdomen was made and hemodynamics obtained following transient occlusions of the abdominal vena cava to vary venous return. Data were collected with the Iworx IX/228S Data Acquisition System and analyzed with Labscribe 2.0 software package from Iworx (Dover, NU). After each experiment mice were euthanized with an overdose of 5% isoflurane, their hearts removed and weighed as previously described [8,14-16].

In addition, total peripheral resistance (TPR) was derived by dividing mean arterial pressure by cardiac output. Cardiac index (CI) was derived by the ratio of cardiac output divided by body weight. The A-V relationship was derived by the ratio of E_a divided by E_{max} . E_{max} was obtained from the slope of the ESPVR obtained following transient occlusions and E_a (a term that incorporates arterial load, TPR, and arterial compliance), was derived from the ratio of the end systolic pressure over stroke volume. Cardiac contractile efficiency (CCE), was derived by the ratio of external work over the pressure volume loop area [8,14].

Quantitative RT-PCR

Total RNA was extracted from the apex of the heart with TRIzol (Invitrogen) and used in a one-step RT-PCR reaction with the SYBR Green RNA Amplification kit (Roche Molecular Biochemical, IN), using the LightCycler thermocycler (Roche Diagnostics). The reaction conditions for the reverse transcriptase were 55°C for 15 min, denaturation at 95°C for 30 sec, followed by four-step PCR amplification for 40-cycles. Samples were normalized

against expression of the large ribosomal protein P0 (Rplp0) to ensure equal loading, as previously described [8].

Gene	Forward primer	Reverse primer	Genebank accession number
β -Myosin heavy chain	AAGGTGAAGGCCTACAAGCG	TTCTGCTTCCACCTAAAGGGC	M74752
Atrial natriuretic factor	TGGAGGAGAAGATGCCGGTA	CGAAGCAGCTGGATCTTCGTAG	K02781
Rplp0	GGCCCTGCACTCTCGCTTTC	TGCCAGGACGCGCTTGT	NM_007475

Statistics

Data are expressed as means \pm standard error (SE). Differences in the means were tested using ANOVA followed by Newman-Keuls post-hoc analysis, where appropriate. Cardiac function data were analyzed using 2-way ANOVA to test the influence of two independent variables: infarct and treatment. An all pairwise multiple comparisons using the Holm-Sidak method was used to test for statistical significance ($P < 0.05$).

Results

Post-MI survival curves showed that injection of MGF E-domain peptide eluting MRS resulted in 100% survival in both 2 and 10 wk post-MI mice, similar to sham operated mice (Fig 1A, B). At 2 week post-MI, there was 20% mortality in the untreated MI group with the greatest incidence of death occurring within the first 2 days. Injection of either empty MRS or MGF E-domain peptide alone resulted in 10% mortality in both groups. At 10 weeks post-MI there was greater mortality in the untreated MI and empty MRS injected groups (33% and 46% respectively), whereas a 100% survival was maintained in the MGF E-domain peptide eluting MRS group.

Initial statistical analysis showed most hemodynamic and functional parameters were depressed in the sham operated controls compared to non-operated control mice, but overall did not get progressively worse with time (Supplemental Table 1). Most noticeable were the significant increases in volumes (ESV and EDV) which impacted ejection fraction (EF), load dependant contractile function ($^{+/-}dp/dt$) and the rate of relaxation (Tau). These data indicate that the rupture of the pericardium and possible tissue damage caused by intramuscular injection was sufficient to depress cardiac function, so subsequent analysis of treatments were made in comparison to sham operated controls at each time point. In addition, analysis of the untreated MI mice compared to non-operated controls showed a significant depression of cardiovascular function that worsened with time post-MI (Supplemental Table 2). This functional decline over time post-MI and the hemodynamic parameters recorded are similar to our previous studies and indicative of mice with infarcts $>45\%$ of the LV [8,14-16].

Load dependent hemodynamic parameters derived in the closed chest configuration from the various groups at 2 wk post-MI are shown Table 1. Overall a decline in cardiac function was evident in the untreated MI group in comparison to sham controls. While volumes did not increase to the same extent as in sham controls, there was a significant increase in EDP.

Furthermore, these untreated MI hearts could not maintain stroke volume and stroke work, which were significantly depressed. Cardiac output and cardiac index also showed signs of further deterioration compared to shams (Table 1). Injection of MGF E-domain peptide eluting MRS led to improvements in a number of hemodynamic parameters such as MAP, ESP, SV, EF, $^{+/-}$ dp/dt, SW and MaxPower relative to untreated MI and were either similar or slightly elevated compared to sham controls. There was a significant improvement in CO, which was probably a result of an improved SV despite similar volumes as untreated MI mice. Mice injected with either the empty MRS or MGF E-domain peptide alone showed no significant improvement relative to untreated MI, indicating that biological activity and protection against degradation of the native MGF E-domain peptide was achieved with the peptide eluting MRS.

A greater number of improvements were noted with MGF E-domain peptide eluting MRS treatment by 10 wk post-MI, in contrast to the 2 wk post-MI groups (Table 2). In comparison to the shams, significantly more functional deterioration had occurred in the untreated 10 wk MI hearts, as evidenced by further dilation of ventricles and decline in ESP, SV, CO, EF, SW, and MaxPower. In addition, contractile function ($^{+/-}$ dp/dt) and relaxation (Tau) were significantly depressed along with the ability to maintain MAP. The MGF E-domain peptide eluting MRS injected mice showed a marked preservation of cardiac function with hearts operating at equivalent levels as sham controls. Mean arterial pressure and ESP were no longer significantly different, as well as load-dependent measurements of cardiac contractility and work (SW, $^{+/-}$ dP/dt, MaxPower) and relaxation (Tau), which were significantly improved relative to 10 wk MI group. Mice injected with the empty MRS showed significantly depressed function compared to shams and were indistinguishable from the untreated 10 wk MI group in most parameters. However, there was a tendency to show less deterioration in ESP, SW, and MaxPower in these hearts suggesting the MRS may impact some aspects of cardiac function.

Cardiac contractility measured following vena cava occlusion was improved in MGF E-domain peptide eluting MRS injected mice compared to untreated 2 wk MI mice. Both the end systolic pressure volume relationship (ESPVR) and preload recruitable stroke work (PRSW) were enhanced compared to 2 wk MI, and were the same as sham controls (Fig 2A). Contractility of hearts injected with empty MRS or peptide alone was depressed and not significantly different than the untreated MI hearts. Analysis of the 10 wk post-MI group revealed a significant decline in function in the untreated MI and empty MRS injected hearts compared to shams (Fig 2B). However, mice injected with the peptide eluting MRS showed no signs of decline and were significantly improved relative to the untreated MI group. Ventricular stiffness measured by the end diastolic pressure volume relationship (EDPVR), revealed an increased stiffness (decreased compliance) in all 2 and 10 wk MI groups, except those injected with the empty MRS at 10 wk post-MI (Fig 2C).

Since the pressure volume area (PVA) has been shown to correlate linearly with oxygen consumption, we examined ventricular mechanoenergetics in both groups of mice [19]. The external work (EW) of the heart was significantly depressed in all the 2 wk MI groups compared to shams, except those injected with MGF E-domain peptide eluting MRS (Fig 3A). As a percent of the PVA, the decline in EW was similar amongst all groups indicating a

decrease in cardiac contractile efficiency, with improvements noted in the MI+EpepMRS treated group only (2 wk sham EW=60% PE=40%, MI EW=61% PE=39%, MI+EpepMRS EW=67% PE=33%, MI+MRS EW=56% PE=64%, MI+Epep EW=60% PE=40%). Analysis of the 10 wk post-MI group showed a similar response in the untreated MI and MI+MRS groups, whereas MI+EpepMRS treatment showed signs of increased efficiency compared to shams (10 wk sham, EW=55%, PE=45%, MI EW=46% PE=54%, MI+EpepMRS EW=74% PE=26%, MI+MRS EW=56% PE=44%), (Fig 3B). To examine further the influence of peptide eluting MRS treatments on global cardiovascular function, the contractile efficiency was plotted against the vascular-to-ventricular coupling ratio and compared to non-operated controls (Fig 3C, D). While these represent derived indexes of ventricular and vascular function, they illustrate how efficiently the ventricle transfers mechanical energy of contraction on to the blood and into the vascular tree. A significant decline in cardiac contractile efficiency (CCE) and increase in the A-V coupling ratio occurred with time in untreated MI mice indicating these hearts were contracting with low efficiency against an increasing vascular impedance. While the MI+MRS treated mice did not show improvement *per se*, they did not get progressively worse suggesting an ability of the MRS to stabilize and limit a further decline in function. In contrast, mice treated with the MI+E peptide eluting MRS showed the greatest improvements even though there was a significant increase in the A-V coupling ratio by 10 wk post-MI. This suggests that while a similar decline in vascular function occurred in these mice, localized delivery of the MGF E-domain peptide to the heart was sufficient to preserve contractile function and delay decompensation.

To determine the effects of MGF E-domain peptide MRS treatment on cardiac remodeling, cardiac mass was examined. Despite the functional decline in the sham operated groups, there was no indication of cardiac hypertrophy based on heart weight to body weight ratio's (HW/BW), as compared to non-operated controls (CTL= 4.45±0.07, 2wk sham= 4.3±0.04, 10wk sham= 4.2±0.1). Conversely, HW/BW ratio was significantly greater in all 2 wk post-MI groups compared to sham control, with signs of attenuation in the MI+E peptide eluting MRS injected group (Fig 4A). In the 10 wk post-MI cohort, there was a significant increase in the HW/BW ratio in untreated MI and MI+MRS treated groups compared to sham (Fig 4A). There was no indication of cardiac hypertrophy in the MI+E peptide eluting MRS treated group, which correlates with the functional improvements. This was also verified by measuring heart weight to tibia length to account for any variation in body weight in the 10 wk post-MI mice (Supplemental table 3).

Expression of the embryonic β -myosin heavy chain isoform (β -MHC) and atrial natriuretic factor (ANF) mRNA in the ventricles are associated with pathologic remodeling in the rodent heart. At 2 wk both β -MHC and ANF mRNA expression was significantly elevated in all MI groups compared to shams, except those treated with the MGF E-domain eluting MRS (Fig 4B, C). A similar increase in expression was observed in the 10wk MI hearts which was attenuated in the MI+empty MRS hearts (Fig 4D, E). However, there was no significant increase noted in the MI+E peptide eluting MRS treated group, indicating the molecular events associated with pathologic remodeling were inhibited.

Discussion

The data presented here show that polymeric PEG-based hydrogel microstructures engineered to be the same size, shape and stiffness as adult cardiac myocytes can be used to protect and elute biologically active native peptides. We show for the first time that this technology permits cardiac restricted delivery of the MGF E-domain peptide to improve contractile function and prevent pathologic remodeling of the heart to increase survival following myocardial infarction.

An immediate consequence of myocardial infarction is the precipitous decline in contractile function due to irreversible cell death of the myocardium caused by ischemia. In order to limit damage growth factors such as IGF-1 are produced by the myocardium and play a role in regulating contractility, hypertrophy, metabolism and apoptosis in the heart. Studies have shown increased IGF-1 mRNA and protein expression in the hearts of animal models following MI [1,9,20]. Myocytes isolated from different regions (border zone and remote region) show increased expression of IGF-1, supporting the view that IGF-1 expression occurs within the cardiac myocytes [21]. To recapitulate the actions of IGF-1 produced by the heart, cardiac restricted expression of IGF-1 in transgenic models has shown it protects the cardiac myocytes from oxidative stress and promotes functional recovery following MI [22,23]. Similar results have also been obtained with cardiac restricted over-expression of the IGF-1 receptor (IGF-1R), emphasizing the importance of IGF-1 and its downstream pathway in protection and functional recovery in response to ischemic injury [24,25].

Recently interest has grown in the function of IGF-1 isoforms expressed in response to injury and the action of their unique E-domains. The mechanism by which the E-domain regions exert their biological effects is unknown, but data from several studies coalesce around modulating the actions of IGF-1. Synergistic activation of the IGF-1R and downstream signaling has been shown to occur with the E-domains and IGF-1 *in vitro* [26,27]. It has also been suggested that the E-domains regulate the IGF-1 extracellular matrix interaction upon secretion, thereby modulating IGF-1 availability within the local environment [28]. In addition, preventing cleavage of the E-domain by mutating proprotein convertase cleavage sites within the IGF-1 propeptide induces different gene expression profiles compared to the mature IGF-1 peptide alone, when expressed in skeletal muscle [29]. Extending this further are data showing sustained expression of IGF-1 isoforms harboring an inactivation mutation in the mature peptide region while leaving expression of the E-domain region intact, is sufficient to stimulate an increase in skeletal muscle mass [30]. Thus, together these genetic approaches investigating the actions of the E-domain region implicate a biological function that may involve modulating aspects of IGF-1 availability and signaling.

The rationale for the use of the MGF isoform E-domain peptide analog to further define the actions of the E-domain region, is several fold. First, the MGF isoform has different temporal dynamics in various tissues compared to the predominant IGF-1Ea isoform, suggesting it plays a role in tissue repair [8-10]. Second, the pattern of alternate splicing to produce the unique carboxyl region of this isoform is conserved between human and non-human primates [31]. Third, the use of the peptide provides a tool to examine potential

actions without the confounding effects of mature IGF-1, which is expressed with most genetic approaches used to date to examine isoform function. Finally, given the accumulating data suggesting that the E-domain region modulates IGF-1 actions, delivery of the peptide may provide a means to augment endogenous IGF-1 without delivery of exogenous IGF-1. Supporting this are studies involving neurologic and cardiac injury models in which delivery of the MGF E-domain peptide exhibits salutary effects [8,11-14]. However, while these studies have shown functional benefits associated with systemic delivery of the stabilized MGF E-domain peptide, they do not exclude the possibility that other circulating factors may be involved. Here we show for the first time that localized delivery of the native E-domain peptide can elicit improvements in cardiac function following MI, indicating that the actions of the peptide are localized to the myocardium.

Overall the data in the present study show many similarities to our prior physiologic studies with systemic delivery of the stabilized MGF E-domain peptide in the mouse MI model [8,14]. Several consistent findings exist in that there is preservation of contractility, attenuation of pathologic hypertrophy and decreased expression of embryonic isoforms. Moreover, analysis of cardiac function at 10 wk post-MI showed systemic delivery of the peptide during the acute phase post-MI produced many similar effects to those found with intramyocardial delivery during the same time-frame [14]. Again, the improvement in contractility and cardiac contractile efficiency appears sufficient to prevent the decompensated stage that occurs in untreated MI hearts. These effects appear to be confined to the heart since the increase in vascular-to-ventricular coupling ratio was essentially the same in both studies. However, a notable difference in this study was the inhibition of cardiac hypertrophy and the associated decrease in embryonic gene expression profiles compared to systemic delivery, which did not lead to inhibition of hypertrophy, but did show decreased ANF expression. Explanations for these differences could be due to the direct action of the peptide with localized delivery compared to a wider biodistribution associated with systemic delivery. Moreover, the combined benefit of the peptide and the actions of the hydrogel MRS may also contribute to the improved effects on cardiac remodeling noted here. While the empty MRS treated group did not show significant improvements post-MI, a noticeable trend was that these hearts stabilized and did not get progressively worse between the time points. In addition, ventricular stiffness during diastole as measured by the EDPVR, was lower than all the other MI groups at 10 wks which was associated with an attenuation of embryonic isoform gene expression. These phenomena could occur if the extent of interstitial fibrosis and increased collagen deposition during scar expansion was affected by the presence of the MRS. The use of the MRS engineered with these specifications was based on previous data showing that the empty MRS can inhibit NIH 3T3 fibroblast proliferation and down regulate expression of myofibroblast markers (collagen I, VI and α -smooth muscle actin) when seeded in a 3D culture system [17]. These studies were recently extended by showing that intramyocardial delivery of the empty MRS alone is sufficient to limit fibrosis to an ischemia-reperfusion model *in vivo* [32]. Moreover, studies examining cardiac myocyte remodeling in 3D cultures showed that the presence of microrods influence cardiac myocyte size, protein content, myofibrillar alignment and gene expression, indicating that the physical cues of the microenvironment can play a significant role in regulating cellular function [33,34].

Consequently, the microscale topographic cues these polymeric structures present and how they regulate cell-cell interactions is the focus of an emerging field aimed at governing cell behavior through tissue engineered constructs and their *in vivo* applications.

The tunable material properties of PEG-based hydrogels have been exploited for tissue repair through delivery of biomolecules due to their good biocompatibility and hydrophilicity [35-37]. Biodegradable poly(D, L-lactic acid) films fabricated with the MGF E-domain peptide chemically bonded to a copolymer have been used in bone tissue engineering, since the MGF E-domain peptide promotes osteoblast activity *in vitro* and bone healing in rabbits *in vivo* [38,39]. Furthermore, intranasal delivery of TAT/MGF E-domain peptide tagged chitosan nanoparticles have been proposed as a potential method to cross the blood brain barrier for delivery of neurotherapeutics [40]. In this context, the MGF E-domain peptide was used as a neuronal cell penetrating peptide to optimize delivery of the biotin-siRNA contained within the nanoparticle. Interestingly, while the authors were able to detect the presence of the biotin-siRNA in the brain within hours of delivery, their biodistribution data in other tissues showed the presence of the biotin-siRNA in the heart. These data corroborate our previously published data showing cellular uptake of an FITC labeled MGFE-domain peptide in a cardiac myocytes which can be inhibited with unlabelled peptide [8]. Thus, in combination with the cell-sized PEG-based MRS this technology functions an injectable delivery platform for sustained release of active biologicals. We acknowledge the limitations of this present study are encompassed by the use of the permanent coronary ligation model, the invasive nature of the delivery approach and a single dose of MRS treatment. However, the use of appropriate control groups allowed for accurate comparisons of the beneficial effects of the MGF E-domain peptide and efficacy of our novel delivery technology.

Conclusions

We demonstrate by integrating novel bioengineering concepts in the development of our technology and physiologic approaches for assessment of function, we can support tissue repair by the release of biologically active peptides. As such, our data showing intramyocardial delivery of the E-domain region of the MGF isoform of IGF-1 represents a feasible strategy to preserve contractile function with therapeutic implications for slowing the progression of heart failure. Furthermore, our approaches also extend to the use and delivery of other therapeutic peptides and compounds to support tissue repair associated with other pathologies and possibly tissue regeneration.

Supplementary Material

Refer to Web version on PubMed Central for supplementary material.

Acknowledgments

This work was supported National Institutes Health, Heart Lung and Blood Institutes R01 HL090523 (PHG). All authors contributed significantly to this work.

References

1. Reiss K, Kajstura J, Zhang X, Li P, Szoke E, Olivetti G, Anversa P. Acute myocardial infarction leads to upregulation of the IGF-1 autocrine system, DNA replication, and nuclear mitotic division in the remaining viable cardiac myocytes. *Exp Cell Res.* 1994; 213:463–72. [PubMed: 7914170]
2. Duerr RL, Huang S, Miraliakbar HR, Clark R, Chien KR, Ross J Jr. Insulin-like growth factor-1 enhances ventricular hypertrophy and function during the onset of experimental cardiac failure. *J Clin Invest.* 1995; 95:619–27. [PubMed: 7860746]
3. Froesch ER, Schmid C, Schwander J, Zapf J. Actions of insulin-like growth factors. *Annu Rev Physiol.* 1985; 47:443–67. [PubMed: 2986538]
4. Russell SM, Spencer EM. Local injections of human or rat growth hormone or of purified human somatomedin-C stimulates unilateral tibial epiphyseal growth in hypophysectomized rats. *Endocrinology.* 1985; 116:2563–7. [PubMed: 4039658]
5. Vetter U, Zapf J, Heit W, Helbing G, Heinze E, Froesch ER, Teller WM. Human fetal and adult chondrocytes. Effect of insulin like growth factors I and II, insulin, and growth hormone on clonal growth. *J Clin Invest.* 1989; 77:1903–8. [PubMed: 3519682]
6. Shimatsu A, Rotwein P. Mosaic evolution of the insulin-like growth factors. Organization, sequence, and expression of the rat insulin-like growth factor I gene. *J Biol Chem.* 1987; 262:7894–900. [PubMed: 3034909]
7. Oberbauer AM. The Regulation of IGF-1 Gene Transcription and Splicing during Development and Aging. *Front Endocrinol.* 2013; 4:39.
8. Mavrommatis E, Shioura KM, Los T, Goldspink PH. The E-domain Region of Mechano-Growth Factor Inhibits Cellular Apoptosis and Preserves Cardiac Function during Myocardial Infarction. *Mol Cell Biochem.* 2013; 381:69–83. [PubMed: 23712705]
9. Philippou A, Papageorgiou E, Bogdanis G, Halapas A, Sourla A, Maridaki M, Pissimissis N, Koutsilieris M. Expression of IGF-1 isoforms after exercise-induced muscle damage in humans: characterization of the MGF E peptide actions in vitro. *In Vivo.* 2002; 23:567–75. [PubMed: 19567392]
10. Hill MA, Goldspink G. Expression and splicing of the insulin-like growth factor gene in rodent muscle is associated with muscle satellite (stem) cell activation following local tissue damage. *J Physiol.* 2003; 549:409–18. [PubMed: 12692175]
11. Carpenter VA, Matthews KG, Devlin GP, Stuart SP, Jensen JA, Conaglen JV, Jeanplong F, Goldspink PH, Yang SY, Goldspink G, Bass JJ, McMahon CD. Mechano-Growth Factor Ameliorates Loss of Cardiac Function in Acute Myocardial Infarction. *Heart Lung Circ.* 2008; 17:33–9. [PubMed: 17581790]
12. Dluzniewska J, Sarnowska A, Beresewicz M, Johnsomn I, Srail SK, Ramesh B, Goldspink G, Gorecki DC, Zablocka B. A strong neuroprotective effect of the autonomous C-terminal peptide of IGF-1 Ec (MGF) in brain ischemia. *FASEB J.* 2005; 19:1896–8. [PubMed: 16144956]
13. Quesada A, Ogi J, Schultz J, Handforth A. C-terminal mechano-growth factor induces heme oxygenase-1-mediated neuroprotection of SH-SY5Y cells via the protein kinase C ϵ /Nrf2 pathway. *J Neurosci Res.* 2011; 89:394–405. [PubMed: 21259326]
14. Shioura KM, Peña JR, Goldspink PH. Administration of a Synthetic Peptide Derived from the E-domain Region of Mechano-Growth Factor Delays Decompensation following Myocardial Infarction. *Int J Cardiovasc Res.* 2014; 3:3.10.4172/2324-8602.1000169
15. Shioura KM, Geenen DL, Goldspink PH. Assessment of Cardiac Function with the Pressure-volume Conductance System Following Myocardial Infarction in Mice. *Am J Physiol Heart Circ Physiol.* 2007; 293:H2870–2877. [PubMed: 17720769]
16. Shioura KM, Geenen DL, Goldspink PH. Sex related differences in cardiac function during the progression to heart failure following myocardial infarction in mice. *Am J Physiol Regul Integr Comp Physiol.* 2008; 5:R528–534.
17. Ayala P, Lopez JI, Desai TA. Microtopographical cues in 3D attenuate fibrotic phenotype and extracellular matrix deposition: implications for tissue regeneration. *Tissue Eng Part A.* 2010; 16:2519–27. [PubMed: 20235832]

18. Doroudian G, Pinney J, Ayala P, Los T, Desai TA, Russell B. Sustained delivery of MGF peptide from microrods attracts stem cells and reduces apoptosis of myocytes. *Biomed Microdevices*. 2014; 16:705–15. [PubMed: 24908137]
19. Suga H. Total Mechanical Energy of a Ventricle Model and Cardiac Oxygen Consumption. *Am J Physiol*. 1979; 236:H498–H505. [PubMed: 426086]
20. Matthews KG, Devlin GP, Conaglen JV, Stuart SP, Mervyn Aitken W, Bass JJ. Changes in IGFs in cardiac tissue following myocardial infarction. *J Endocrinol*. 1999; 163:433–45. [PubMed: 10588817]
21. Loennechen JP, Støylen A, Beisvag V, Wisløff U, Ellingsen O. Regional expression of endothelin-1, ANP, IGF-1, and LV wall stress in the infarcted rat heart. *Am J Physiol Heart Circ Physiol*. 2001; 280:H2902–10. [PubMed: 11356651]
22. Li Q, Li B, Wang X, Leri A, Jana KP, Liu Y, Kajstura J, Baserga R, Anversa P. Overexpression of insulin-like growth factor-1 in mice protects from myocyte death after infarction, attenuating ventricular dilation, wall stress, and cardiac hypertrophy. *J Clin Invest*. 1997; 100:1991–1999. [PubMed: 9329962]
23. Santini MP, Tsao L, Monassier L, Theodoropoulos C, Carter J, Lara-Pezzi E, Slonimsky E, Salimova E, Delafontaine P, Song SY, Bergmann M, Freund C, Suzuki K, Rosenthal N. Enhancing repair of the mammalian heart. *Circ Res*. 2007; 100:1732–1740. [PubMed: 17525368]
24. McMullen JR, Shioi T, Huang WY, Zhang L, Tarnavski O, Bisping E, Schinke M, Kong S, Sherwood MC, Brown J, Riggi L, Kang PM, Izumo S. The insulin-like growth factor 1 receptor induces physiological heart growth via the phosphoinositide 3-kinase(p110alpha) pathway. *J Biol Chem*. 2004; 279:4782–93. [PubMed: 14597618]
25. Lin RC, Weeks KL, Gao XM, Williams RB, Bernardo BC, Kiriazis H, Matthews VB, Woodcock EA, Bouwman RD, Mollica JP, Speirs HJ, Dawes IW, Daly RJ, Shioi T, Izumo S, Febbraio MA, Du XJ, McMullen JR. PI3K(p110 alpha) protects against myocardial infarction-induced heart failure: identification of PI3K-regulated miRNA and mRNA. *Arterioscler Thromb Vasc Biol*. 2010; 30:724–32. [PubMed: 20237330]
26. Durzy ska J, Philippou A, Brisson BK, Nguyen-McCarty M, Barton ER. The pro-forms of insulin-like growth factor I (IGF-I) are predominant in skeletal muscle and alter IGF-I receptor activation. *Endocrinology*. 2013; 154:1215–24. [PubMed: 23407451]
27. Brisson BK, Barton ER. Insulin-like growth factor-I E-peptide activity is dependent on the IGF-I receptor. *PLoS One*. 2012; 7:e45588. [PubMed: 23029120]
28. Hede MS, Salimova E, Piszczek A, Perlas E, Winn N, Nastasi T, Rosenthal N. E-peptides control bioavailability of IGF-1. *PLoS One*. 2012; 7:e51152. [PubMed: 23251442]
29. Barton ER, DeMeo J, Lei H. The insulin-like growth factor (IGF)-I E-peptides are required for isoform-specific gene expression and muscle hypertrophy after local IGF-I production. *J Appl Physiol*. 2010; 108:1069–1076. [PubMed: 20133429]
30. Brisson BK, Spinazzola J, Park S, Barton ER. Viral expression of insulin-like growth factor I E-peptides increases skeletal muscle mass but at the expense of strength. *Am J Physiol Endocrinol Metab*. 2014; 306:E965–74. [PubMed: 24569593]
31. Wallis M. New insulin-like growth factor (IGF)-precursor sequences from mammalian genomes: the molecular evolution of IGFs and associated peptides in primates. *Growth Horm IGF Res*. 2009; 1:12–23. [PubMed: 18571449]
32. Pinney JR, Du KT, Ayala P, Fang Q, Sievers RE, Chew P, Delrosario L, Lee RJ, Desai TA. Discrete microstructural cues for the attenuation of fibrosis following myocardial infarction. *Biomaterials*. 2014; 35:8820–8828. [PubMed: 25047625]
33. Curtis MW, Sharma S, Desai TA, Russell B. Hypertrophy, gene expression, and beating of neonatal cardiac myocytes are affected by microdomain heterogeneity in 3D. *Biomed Microdevices*. 2010; 12:1073–85. [PubMed: 20668947]
34. Curtis MW, Budyn E, Desai TA, Samarel AM, Russell B. Microdomain heterogeneity in 3D affects the mechanics of neonatal cardiac myocyte contraction. *Biomech Model Mechanobiol*. 2013; 12:95–109. [PubMed: 22407215]
35. Kloxin AM, Kasko AM, Salinas CN, Anseth KS. Photodegradable hydrogels for dynamic tuning of physical and chemical properties. *Science*. 324:59–63. 2009. [PubMed: 19342581]

36. Lin CC, Anseth KS. PEG hydrogels for the controlled release of biomolecules in regenerative medicine. *Pharm Res.* 2009; 26:631–43. [PubMed: 19089601]
37. Lin CC, Anseth KS. Glucagon-like peptide-1 functionalized PEG hydrogels promote survival and function of encapsulated pancreatic beta-cells. *Biomacromolecules.* 2009; 10:2460–7. [PubMed: 19586041]
38. Deng M, Zhang B, Wang K, Liu F, Xiao H, Zhao J, Liu P, Li Y, Lin F, Wang Y. Mechano growth factor E peptide promotes osteoblasts proliferation and bone-defect healing in rabbits. *Int Orthop.* 2011; 35:1099–106. [PubMed: 21057789]
39. Li Y, Zhang B, Ruan C, Wang P, Sun J, Pan J, Wang Y. Synthesis, characterization, and biocompatibility of a novel biomimetic material based on MGF-Ct24E modified poly(D, L-lactic acid). *J Biomed Mater Res A.* 2012; 100:3496–502. [PubMed: 22941771]
40. Malhotra M, Tomaro-Duchesneau C, Saha S, Prakash S. Intranasal, siRNA Delivery to the Brain by TAT/MGF Tagged PEGylated Chitosan Nanoparticles. *Journal of Pharmaceutics.* 2013 Article ID 812387, 10 pages. 10.1155/2013/812387

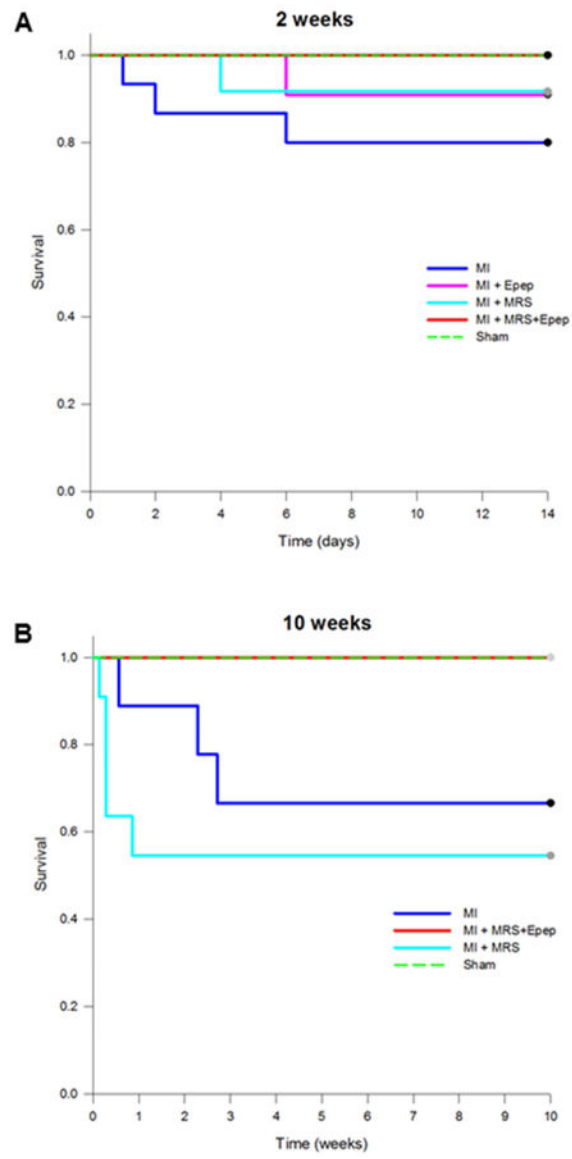


Figure 1. Kaplan-Meier survival curves for 2 and 10 wk post-MI mice, with and without treatments.

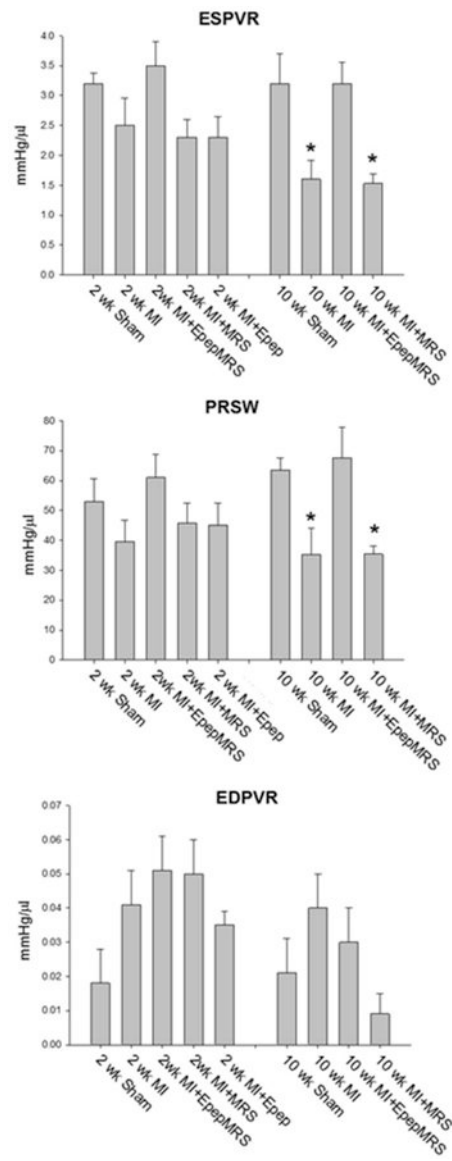


Figure 2.

Cardiac contractility based on pressure-volume loop measurements collected during transient occlusion of abdominal vena cava in 2 and 10 wk post-MI mice. **A.** ESPVR-end systolic pressure volume relationship. **B.** PRSW-preload recruitable stroke work. **C.** EDPVR-end diastolic pressure volume relationship. Data are means \pm S.E., * $P < 0.05$ vs. 10 wk sham.

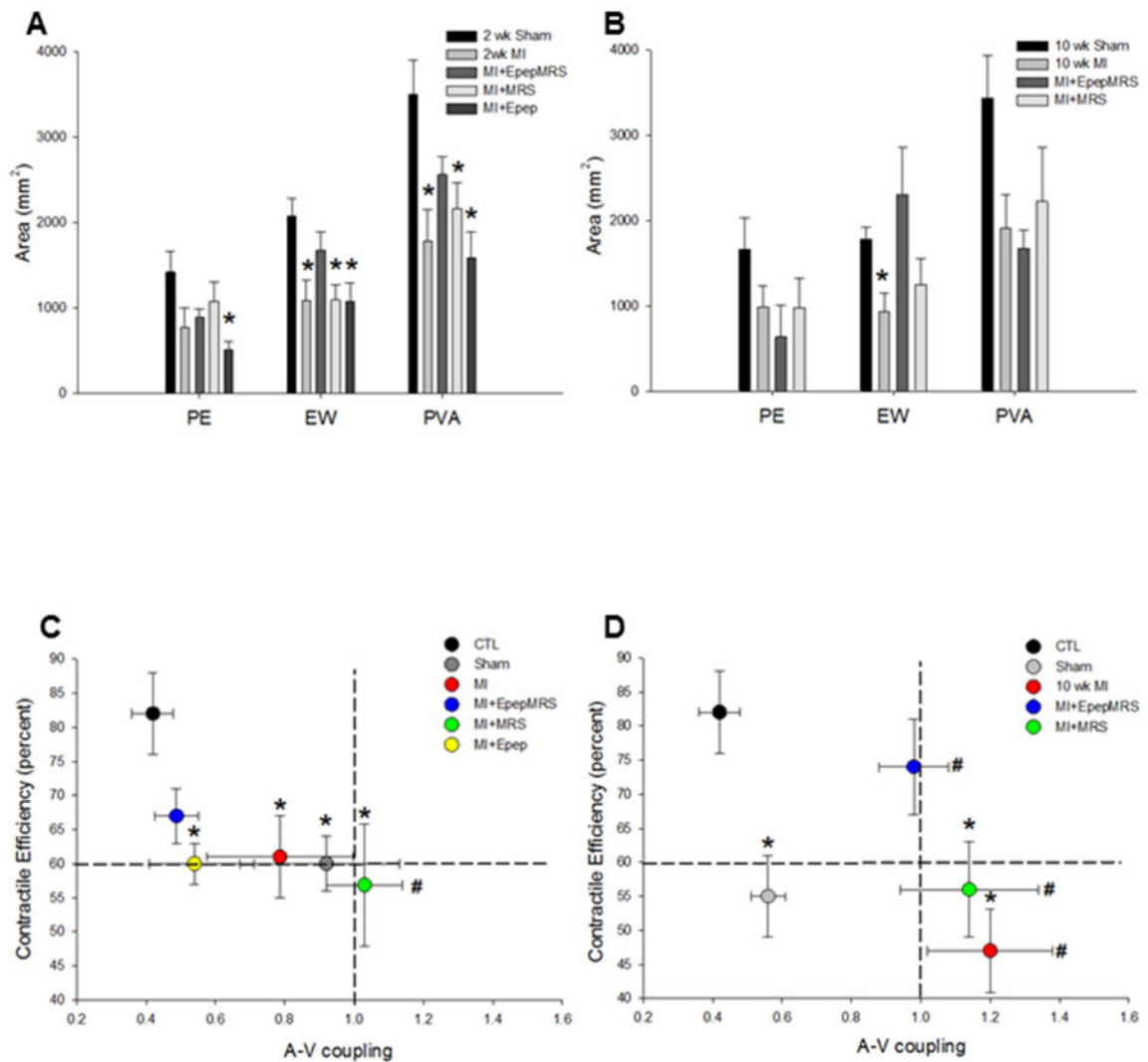


Figure 3.

A&B. Ventricular mechanoenergetics based on PV loop area in 2 and 10 wk post-MI with and without systemic delivery of MGF E-domain peptide. Data are means \pm S.E.M, $*P < 0.05$ vs shams. **C&D.** Integrated cardiovascular function represented by plotting Cardiac Contractile efficiency vs. A-V coupling relationship in non-operated controls and treated mice. Data are means \pm S.E., $*P < 0.05$ vs. CTL CCE and $\#P < 0.05$ vs. CTL A-V coupling.

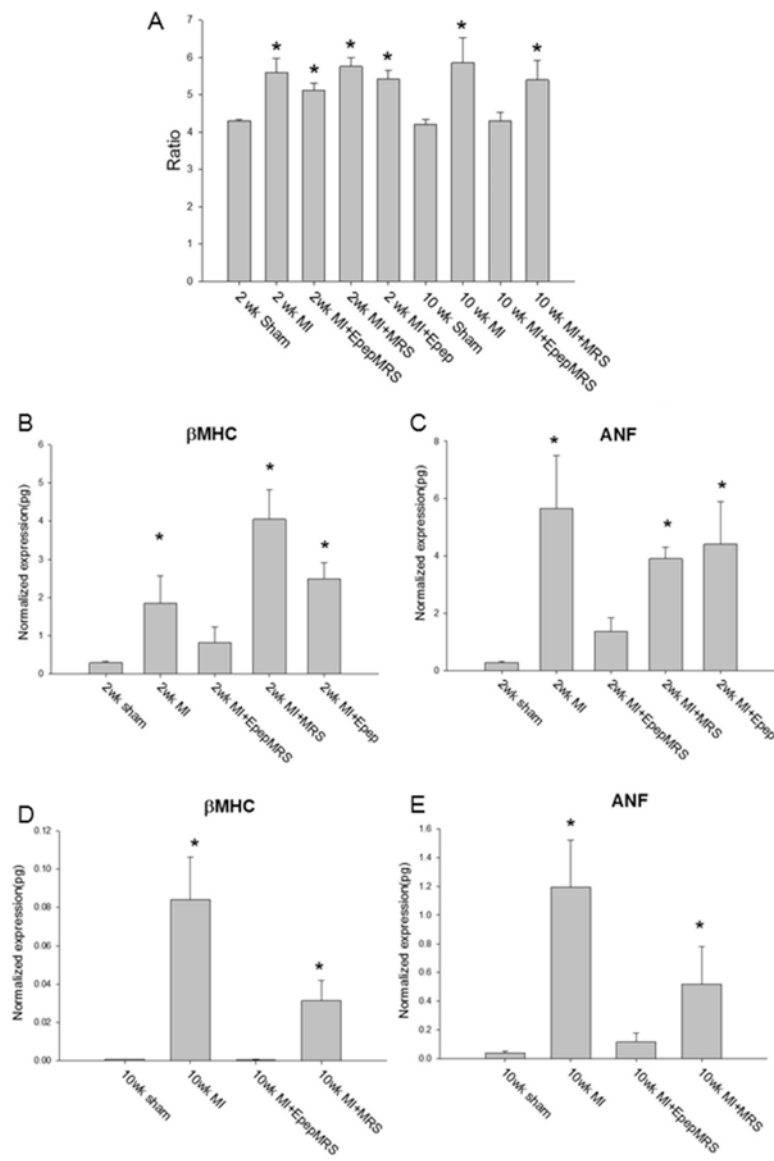


Figure 4. Cardiac mass and quantification of gene expression analysis. **A.** Heart weight to body weight ratio. **B, C.** β -myosin heavy chain isoform expression and atrial natriuretic factor (ANF) expression in 2wk post-MI mice. **D, E.** β -myosin heavy chain isoform expression and atrial natriuretic factor (ANF) expression in 10wk post-MI mice. Data are means \pm S.E., * $P < 0.05$ vs. sham.

Table 1

Cardiac function with E-domain peptide eluting MRS and empty MRS treatments in mice at 2 wks post-MI. Pressure-volume loop measurements in the closed chest configuration. HR-heart rate (*beats per minute*), MAP-mean arterial pressure (*mmHg*), ESP-end-systolic pressure (*mmHg*), EDP-end-diastolic pressure (*mmHg*), ESV-end systolic volume (μ l), EDV-end diastolic volume (μ l), SV-stroke volume (μ l), CO-cardiac output (μ l/min), CI-cardiac index (μ l/min/g), EF-ejection fraction (%), SW-stroke work (*mmHg*/ μ l), dP/dt_{max} -maximum first derivative of change in systolic pressure with respect to time (*mmHg/sec*), dP/dt_{min} -maximum first derivative of change in diastolic pressure with respect to time (*mmHg/sec*), Tau-Glantz-time constant of fall in ventricular pressure by Glantz method (*msec*), MaxPower-maximum power (*mWatts*), TPR-total peripheral resistance (*mmHg*/ μ l/min).

Group Parameter	2 wk Sham	2 wk MI	MI+Epeptide MRS	MI+MRS	MI+Epeptide
HR	472±8.8	488±11.5	504.8±16.7	490.5±11.5	488.7±10.4
MAP	50±3.7	54.3±3	58±2.2	54.3±3	50.5±2.7
ESP	72.1±5.2	75.3±5.9	82.5±3	76±3.8	72±4.2
EDP	1.67±0.1	11.5±1.6*	9.5±1.6*	10.74±2.3*	7.4±2.5*
ESV	35.6±2.5	20.6±3.9*	17.5±2.5*	28.7±5	18.3±4.5*
EDV	61.2±3	37.2±7*	40.0±2.6*	40.9±5.4*	34.7±4.7*
SV	25.6±1.2	16.2±3.1*	23.5±1.7	20.3±1.8	16.6±3*
CO	11602.4±335.6	7799.2±545	11852.2±931.3†	10055.9±1094.7	8038.3±1494.6
CI	151.7±5	126.7±8	146±9.8	123.5±10.6	140±14.7
EF	42±1.7	42.1±2.6	58.3±4.3	43.6±4.8	48.4±8.5
SW	2082.8±199.6	1029±229.6*	1678.3±215	1092.7±177*	1072.5±223.8*
dP/dt_{max}	4015.8±523.7	4581.5±583	5573±420.8	4705±510	4447.5±525.6
dP/dt_{min}	-4444.5±599	-4734.8±726	-5783.9±363	-4769.4±491	-4812.1±560.8
Tau-G	11.7±0.75	10.7±1.4	8.8±0.6	9.9±0.8	9.4±0.4
MaxPower	188947.7±42581	227440±52738	334165±36405.2	270026±42412.6	229866±37517.7
TPR	4.2±0.4	5.9±0.6	5.2±0.65	5.7±0.7	5.3±0.3

* $P < 0.05$ vs. Sham.

† $P < 0.05$ vs. 2 wk MI (n=7-8 per group).

Table 2

Cardiac function with E-domain peptide eluting MRS and empty MRS treatments in mice at 10 wks post-MI. Pressure-volume loop measurements in the closed chest configuration. HR-heart rate (*beats per minute*), MAP-mean arterial pressure (*mmHg*), ESP-end-systolic pressure (*mmHg*), EDP-end-diastolic pressure (*mmHg*), ESV-end systolic volume (μ l), EDV-end diastolic volume (μ l), SV-stroke volume (μ l), CO-cardiac output (μ l/min), CI-cardiac index (μ l/min/g), EF-ejection fraction (%), SW-stroke work (*mmHg*/ μ l), dP/dt_{max} -maximum first derivative of change in systolic pressure with respect to time (*mmHg/sec*), dP/dt_{min} -maximum first derivative of change in diastolic pressure with respect to time (*mmHg/sec*), Tau-Glantz-time constant of fall in ventricular pressure by Glantz method (*msec*), MaxPower-maximum power (*mWatts*), TPR-total peripheral resistance (*mmHg*/ μ l/min).

Group Parameter	Sham	10 wk MI	MI+Epeptide MRS	MI+MRS
HR	510.4±21.3	450±19.8	499.5±22.5	455.6±28
MAP	54±3.4	40.2±3.8*	56±5.5 [†]	49.4±0.9
ESP	76±4.5	56±6	74.4±8.4	72.6±1.5
EDP	4±1.8	2.9±0.6	5.69±1	3±0.75
ESV	33.2±4.2	44.5±10.8	18.8±4.7 [†]	41.9±8.9
EDV	54.2±5	60.2±12.6	38.6±8.2	59.6±11.3
SV	21±1.3	15.6±2	19.8±3.4	17.6±3
CO	10622.6±322.4	7109.6±1106*	9742.2±1606	7714.8±856*
CI	168.8±10.6	152.3±15.4	151±7.8	143.5±12.4
EF	40.4±2.8	27.9±2.3*	52.5±3.3* [†]	31±3.4*
SW	1777.9±146.2	924.9±222.2*	1670.8±211.7	1243.3±309.5
dP/dt_{max}	5350.5±462.2	3036.5±251.3*	5598.5±895.6 [†]	3806±158
dP/dt_{min}	-5331.7±428.7	-3028.6±365.6*	-5484.4±847.8 [†]	-4211.7±167.6
Tau-G	10.3±1.3	17.2±2.4*	9.8±1.4 [†]	13.4±1
MaxPower	294508.5±43464.8	117937.8±17734*	337792.7±82960 [†]	169582.2±8421
TPR	5.1±0.4	6±0.65	6.2±1.2	6.7±0.65

* $P < 0.05$ vs. Sham,

[†] $P < 0.05$ vs. 10 wk MI (n=5-6 per group).